Performance Analysis of Antenna-relay Selection in CNOMA Systems under Practical Impairments

Menaa Saber and Khelil Abdellatif

Echahid Hamma Lakhdar University, El-Oued, Algeria

https://doi.org/10.26636/jtit.2024.3.1589

Abstract — Selection strategies prove to be a valuable approach in mitigating complexity associated with antenna selection (AS) and relay selection (RS), optimizing signal transmission through a streamlined number of antennas/relays, and enhancing overall system performance. This paper offers a comprehensive analysis, deriving closed-form expressions for the outage probability (OP) and throughput in proposed scenarios that leverage the best relay selection (BRS) and transmit antenna selection (TAS) protocol for cooperative non-orthogonal multiple access (CNOMA), along with partial relay selection (PRS) and TAS protocol for CNOMA. The study extends to Rayleigh fading channels, considering practical impairments such as successful interference cancellation (SIC) error, channel estimation error (CEE), and feedback delay error. In comparing the proposed system to conventional CNOMA, our findings highlight the substantial impact of SIC, CEE, and feedback delay imperfections on the performance of both proposed scenarios. Notably, the application of BRS-based TAS protocol outperforms PRS-based TAS in terms of OP and throughput. The close alignment between analytical, asymptotic, and simulation results attests to the credibility of conducted analysis.

Keywords — channel estimation error, CNOMA, outage probability, relay selection, transmit antenna selection

1. Introduction

Non-orthogonal multiple access (NOMA) positions itself as a transformative technology with the potential to shape the landscape of B5G and 6G networks due to its capacity to significantly boost network capacity by optimizing the utilization of scarce spectrum resources [1], [2].

In power-domain NOMA, multiple users are served on the same time-frequency resources [3]. For that, downlink information is efficiently broadcasted using superposition coding (SC) at the base station (BS). Subsequently, successive interference cancellation (SIC) is employed at the users to eliminate multiuser interferences [4].

Recently, there has been a significant gain in interest regarding the utilization of NOMA in cooperative communication for 5G and beyond deployment scenarios [5]. This increased attention is driven by the inherent advantages of cooperative relaying strategies, which include expanded coverage, improved reliability, and effective mitigation of challenges arising from multipath propagation [6].

In relay communication, two widely recognized protocols are employed: the decode-and-forward (DF), in which the relay decodes and re-encodes the information signal before forwarding, and the amplify-and-forward (AF), where the relay amplifies the received signal from the source and transmits it directly to the destination [7].

To enhance the performance of the NOMA system, some studies have explored the combined utilization of NOMA and cooperative communication. In [8], the authors examined a downlink NOMA system with cooperative full-duplex (FD) relaying, employing the near user as a relay for the far user. They derived closed-form expressions for the outage probability (OP) and ergodic sum rate (ESR), considering both fixed power allocations and optimal power allocations aimed at minimizing the OP, as well, the OP performance in a downlink CNOMA with an AF relay [9].

The authors in [10], developed novel closed-form expressions for the bit error rates (BER) of full-duplex cooperative NOMA (FD-CNOMA) systems in the presence of imperfect SIC and residual self-interference (RSI). The authors of [11] have investigated a hybrid relaying scheme, that switches between full and half duplex (FD/HD) to improve the performance of the DF CNOMA system for two users and multi-users [12].

Additionally, the investigation in [13] focuses on evaluating the OP and ESR of an FD/HD coordinated direct and DF-based relay scheme in a NOMA system. This analysis specifically considers scenarios with imperfections in CSI and SIC.

To enhance the coverage and performance for the far user, a proposed scheme in [14] involves utilizing a multi-hop DF relay-aided NOMA (MH-DF-R-NOMA). This scheme includes deriving closed-form expressions for BER and OP in the presence of imperfect SIC and CSI.

While, CNOMA offers benefits like increased spectral efficiency and broader coverage, it also presents challenges such as complexity, interference management, varying channel conditions, limited coverage, power allocation, synchronization issues, and inaccuracies in channel estimation. Addressing these drawbacks is imperative to fully harness the potential of CNOMA in the context of 5G and 6G networks.

To address the drawbacks of CNOMA, relay selection (RS) presents numerous advantages over conventional CNOMA

systems. These include heightened reliability, expanded coverage, enhanced throughput, flexible network deployment options, and improved energy efficiency. The advantages position relay selection as a valuable technique for enhancing the performance and efficacy of 5G and 6G systems.

The impact of RS strategy on the performance of cooperative NOMA is examined to reach the minimal OP across all possible RS schemes and meet the quality of service (QoS) criteria for both users [15]. The authors in [16], delves into the performance analysis of OP and the sum rate of NOMA schemes within AF relay systems considering partial relay selection (PRS). Furthermore, regarding the best relay selection (BRS) considered in [17], the authors analyzed the OP of the optimal RS schemes for cooperative downlink NOMA, considering both fixed and adaptive power allocations (PAs) at the relays, respectively. The OP performance of a dual-hop multi-relay NOMA system using a DF scheme over Nakagami-m fading channels is investigated in [18].

In [19], the authors analyzed the secrecy outage performance for a NOMA network assisted by multiple relays operating over Nakagami-m fading channels, utilizing relay selection. The authors in [20], investigate the analysis of BER performance for both AF and DF relay selection in cooperative NOMA systems over Rayleigh fading channels. Indeed, the AF-assisted max-min relay selection method exhibits superior performance for the far user compared to the DF relay. The implementation of BRS in the downlink scenario of NOMA-based cognitive relay networks (NCRNs) is investigated under the assumption of Rayleigh fading channels in [21].

Beyond the contributions of cooperative communications to enhancing NOMA system performance, researchers suggest the implementation of multiple-input multiple-output (MIMO) techniques to ensure these improvements. Considering that MIMO techniques entail higher complexity and power consumption, the strategy of antenna selection (AS) is deemed a robust option to ensure the desired performance [22].

According to AS techniques, three main protocols are widely known, namely: transmit antenna selection (TAS) [23], receive antenna selection (RAS) [24], and joint transmit and receive antenna selection (JTRAS) [25]. The authors in [26] investigated three NOMA downlink models, including a single-input-single-output (SISO) scenario featuring a single antenna, a multi-input-single-output (MISO) scenario, and a MIMO scenario. The TAS protocol was employed in all scenarios. The authors conducted a comparison of the OP and system throughput, considering all users over Rayleigh fading channels.

In [27], the researchers introduced AS for an FD-CNOMA system to maximize the end-to-end signal-to-interference-plus-noise ratio (SINR) for both the near and far users. This involved employing TAS/RAS protocols at the relay. The performance was characterized in terms of OP and ESR. A comprehensive analysis of the OP performance for two hybrid AS schemes, namely TAS and maximal ratio combining (MRC) at the first hop, as well as JTRAS at the second hop, in a MIMO-NOMA based downlink AF relaying network. The analysis considers the impact of channel estimation error (CEE) and feedback delay over Nakagami-m fading channels [28].

In addition, new combined antenna selection strategies, such as max-max-max and max-min-max, have been developed in [29]. Nevertheless, the max-max-max and max-min-max schemes have the common goal of enhancing the stronger and weaker user, respectively. Furthermore, the impact of hardware impairments (HWI) on the uplink SIMO CNOMA (SIMO-CNOMA) using BRS under SIC and CSI imperfections is examined in terms of OP and system throughput in [30].

Therefore, employing the TAS protocol as a MIMO technique in conventional CNOMA systems yields numerous advantages. These encompass heightened diversity, augmented spectral efficiency, enhanced throughput, reduced interference, and enhanced deployment flexibility.

Drawing from the aforementioned literature, CNOMA studies have predominantly focused on single-relay scenarios, often overlooking factors like imperfect SIC, CEE, and feedback delay. Moreover, investigations rarely delve into the joint application of RS and TAS within CNOMA frameworks. Consequently, the integration of RS and TAS protocols into CNOMA systems while addressing practical challenges such as SIC, CEE, and feedback delay remains largely unexplored. This paper fills this gap by evaluating and analyzing the performance of CNOMA systems using schemes that combine best relay selection with TAS (BRS-TAS CNOMA) and partial relay selection with TAS (PRS-TAS CNOMA), with a focus on OP and throughput performance. Therefore, the primary contributions of this study are outlined as follows:

- We investigate a realistic downlink CNOMA scheme influenced by SIC, CEE, and feedback delay. The study includes different scenarios with multiple relays and antennas, employing the RS technique and the integration of the TAS protocol to improve performance. The transmitting base station (BS) and relays are equipped with multiple antennas, while single antennas are employed at the reception.
- Exact integral expressions for the OP and throughput of all considered scenarios are derived, considering SIC, CEE, and feedback delay imperfections. These expressions are validated through both asymptotic analysis using the

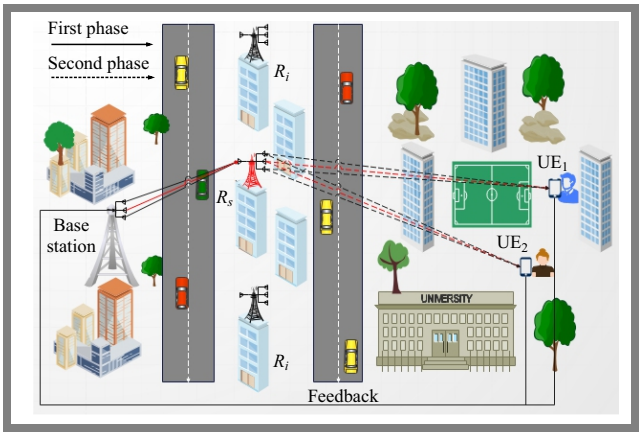

Fig. 1. The concept of system model.

McLaurin series expansion and simulations carried out with computer simulation.

- The impact of key system parameters on the OP and throughput performance is evaluated based on the obtained analytical expressions. These parameters include the number of relays and antennas, the distance between the relay and the base station, the power allocation factor, and practical impairments.
- A performance comparison between the analyzed schemes and their HD relay-aided NOMA system counterpart is provided.
- Finally, numerical results show that the systems under study in the high SNR region are limited by practical constraints, as indicated by the presence of an error floor (EF). Increasing the number of antennas and relays helps reduce these effects.

The rest of the paper is organized as follows: In Section 2, we delve into the MISO-NOMA system utilizing the TAS protocol, exploring both PRS-TAS CNOMA and BRS-TAS CNOMA scenarios while considering imperfections like SIC error, CEE, and feedback delay, taking conventional CNOMA as a benchmark. Section 3 provides a detailed derivation of closed-form expressions for OP in the investigated system. Numerical and simulation results are then presented in Section 4. The paper concludes with Section 5, summarizing the key findings and insights.

2. System Model

Here, we examine the downlink CNOMA system comprising a base station, N relays, and two users: a far user UE_1 and a near user UE_2. As shown in Fig. 1, the BS and relays are equipped with N_t transmit antennas, while each user and relay use a single receiving antenna, resulting in a two-hop communication setup using the TAS scheme. So, the TAS scheme is applied in the two hops, ensuring that N_t at both the BS and relay offers the highest SNR, respectively.

To represent this system under the influence of imperfect SIC and imperfect CSI including CEE and feedback delay, first some notations and definitions are introduced.

$h_{j.SR_i}$ and $h_{j.R_iD}$ are the $N_t \times 1$ fading channel coefficients vector of both hops between the BS–R and R–UE_j, respectively, modeled as a complex Gaussian random variable:

$$h_{j.SR_i} \sim CN\left(0, \sigma^2_{j.I}\right)$$

and

$$h_{j.R_iD} \sim CN\left(0, \sigma^2_{j.II}\right) \ .$$

The variances are defined as:

$$\sigma^2_{j.SR_i} = E\left\{|h_{j.SR_i}|^2\right\}$$

and

$$\sigma^2_{j.R_iD} = E\left\{|h_{j.R_iD}|^2\right\} \ ,$$

with $j = 1, 2$.

$\hat{h}_{j.SR_i}$ and $\hat{h}_{j.R_iD}$ are the $N_t \times 1$ estimated channel coefficients vector of the two-hops can be expressed by:

$$\hat{h}_{j.SR_i} = h_{j.SR_i} - \kappa_{j.I}$$

and

$$\hat{h}_{j.R_iD} = h_{j.R_iD} - \kappa_{j.II} \, ,$$

where $\kappa_{j.I}$ and $\kappa_{j.II}$ are the CEE independent of $\hat{h}_{j.SR_i}$ and $\hat{h}_{j.R_iD}$ and modelled as:

$$\kappa_{j.I} \sim CN\left(0, \sigma^2_{\kappa_{j.I}}\right) \ ,$$

$$\kappa_{j.II} \sim CN\left(0, \sigma^2_{\kappa_{j.II}}\right) \ .$$

The variances are defined as:

$$\sigma^2_{\kappa_{j.I}} = \sigma^2_{j.SR_i} - \widehat{\sigma}^2_{j.SR_i} \ , \ \sigma^2_{\kappa_{j.II}} = \sigma^2_{j.R_iD} - \widehat{\sigma}^2_{j.R_iD},$$

where:

$\widehat{\sigma}^2_{j.SR_i} = E\left\{\left|\widehat{h}_{j.SR_i}\right|^2\right\}$ and $\widehat{\sigma}^2_{j.R_iD} = E\left\{\left|\widehat{h}_{j.R_iD}\right|^2\right\}$ are the variances of $\widehat{h}_{j.SR_i}$ and $\widehat{h}_{j.R_iD}$, respectively, with $j = 1, 2$.

$\widehat{h}^{(\tau)}_{j.SR_i}$ and $\widehat{h}^{(\tau)}_{j.R_iD}$ are the $N_t \times 1$ feedback delayed of the estimated channels vector of $\hat{h}_{j.SR_i}$ and $\hat{h}_{j.R_iD}$ for the two-hops are defined as:

$\hat{h}_{j.SR_i} = \rho\widehat{h}^{(\tau)}_{j.SR_i} + e_{fd_{j.I}}$ and $\hat{h}_{j.R_iD} = \rho\widehat{h}^{(\tau)}_{j.R_iD} + e_{fd_{j.II}}$, where $e_{fd_{j.I}}$ and $e_{fd_{j.II}}$ are the feedback error of the two-hops modelled as:

$e_{fd_{j.I}} \sim CN\left(0, \sigma^2_{fd_{j.I}}\right)$ and $e_{fd_{j.II}} \sim CN\left(0, \sigma^2_{fd_{j.II}}\right)$, which:

$$\sigma^2_{fd_{j.I}} = (1 - \rho_{j.I})\,\widehat{\sigma}^2_{j.SR_i} \, ,$$

$$\sigma^2_{fd_{j.II}} = (1 - \rho_{j.II})\,\widehat{\sigma}^2_{j.R_iD} \, ,$$

$$\rho = J_0(2\pi f_d \tau), \ \ 0 < \rho < 1 \, ,$$

ρ and $f_d\tau$ represents the time correlation coefficient and the normalized Doppler frequency, respectively.

We assume $e_{j.fd}$ and κ_j of the two hops are independent random variables, we define a new error for both hops:

$e_{j.I} = \kappa_{j.I} + e_{fd_{j.I}}$ and $e_{j.II} = \kappa_{j.II} + e_{fd_{j.II}}$,

then

$e_{j.I} \sim CN\left(0, \sigma^2_{e_{j.I}}\right)$ and $e_{j.II} \sim CN\left(0, \sigma^2_{e_{j.II}}\right)$,

where $\sigma^2_{e_{j.I}} = \sigma^2_{\kappa_{j.I}} + \sigma^2_{fd_{j.I}}$ and $\sigma^2_{e_{j.II}} = \sigma^2_{\kappa_{j.II}} + \sigma^2_{fd_{j.II}}$ are the variances of each element in the error term $e_{j.I}$ and $e_{j.II}$, respectively.

To simplify the calculation, we make the assumption:

$$\sigma^2_{\kappa_I} = \sigma^2_{\kappa_{j.I}} \ , \ \sigma^2_{\kappa_{II}} = \sigma^2_{\kappa_{j.II}} \, ,$$

$$\sigma^2_{fd_I} = \sigma^2_{fd_{j.I}} \text{ and } \sigma^2_{fd_{II}} = \sigma^2_{fd_{j.II}} \, .$$

Applying the TAS scheme in the two hops, a transmit antenna, denoted as $\widetilde{t}$, is selected at both the BS and relay. This selection is based on having the maximum sum of squared channel gains between the receiver antennas of the relay and the users. So, the selected transmit antenna criteria for the two-hop is given by:

$$\widetilde{t} = \underset{1<t<N_t}{\arg\max} |h_t|^2. \tag{1}$$

In the best relay selection (BRS) scheme, the optimal relay is selected based on maximizing the minimum SINR between

the source-to-relay link ($S - R_l$) and the relay-to-UE$_j$ link. This selection criteria is expressed as:

$$R_s = \underset{1<l<L}{\arg\max} \left\{ \min \left(\gamma_{SR_i}, \gamma_{R_i D} \right) \right\}. \tag{2}$$

A partial relay selection (PRS) scheme is performed for one hop only, wherein the relay is chosen based on the CSI of each hop. The selection criteria is given as:

$$R_s = \underset{1<l<L}{\arg\max} \left\{ \left(\gamma_{SR_i} \right) \right\}, \tag{3}$$

and

$$R_s = \underset{1<l<L}{\arg\max} \left\{ \left(\gamma_{R_i D} \right) \right\}. \tag{4}$$

In the first hop of communication, the BS transmits a superimposed signal $x = \sum_{j=1}^{2} \sqrt{P_t \alpha_j} x_j$ to the relay, where x_j are the messages of UE$_j$, P_t denotes the BS transmit power and the coefficients α_j satisfy the conditions:

$\sum_{j=1}^{2} \alpha_j = 1$ and $\alpha_1 > \alpha_2$ leading to $|h_{1.SR_i}|^2 < |h_{2.SR_i}|^2$.

The received signal by the relay is given as:

$$y_r = \left(\rho \widehat{\widetilde{h}}^{(\tau)}_{j.SR_i} + e_I \right) \sum_{j=1}^{2} \sqrt{P_t \alpha_j} x_j + n_r, \tag{5}$$

where n_r is the additive white Gaussian noise (AWGN) $n_r \sim CN\left(0, N_o\right)$.

The received SINRs for x_1 and x_2 at the relay are given, respectively by:

$$\gamma_1^{SR_i} = \frac{\alpha_1 \gamma_0 \left| \widehat{\widetilde{h}}^{(\tau)}_{1.SR_i} \right|^2}{\alpha_2 \gamma_0 \left| \widehat{\widetilde{h}}^{(\tau)}_{1.SR_i} \right|^2 + \frac{\gamma_0}{\rho_I^2} \left(\sigma_{\kappa_I}^2 + \sigma_{fd_I}^2 \right) + \frac{1}{\rho_I^2}}, \tag{6}$$

and

$$\gamma_2^{SR_i} = \frac{\alpha_2 \gamma_0 \left| \widehat{\widetilde{h}}^{(\tau)}_{2.SR_i} \right|^2}{\alpha_1 \gamma_0 \xi \left| \widehat{\widetilde{h}}^{(\tau)}_{2.SR_i} \right|^2 + \frac{\gamma_0}{\rho_I^2} \left(\sigma_{\kappa_I}^2 + \sigma_{fd_I}^2 \right) + \frac{1}{\rho_I^2}}, \tag{7}$$

where ξ denotes the residual SIC factor and $\gamma_0 = \frac{P_t}{N_0}$ is the transmit SNR.

In the second hop of communication, the RS transmits a superimposed signal $x = \sum_{j=1}^{2} \sqrt{P_r \alpha_j} x_j$ to the users, where x_j are the messages of UE$_j$, P_r denotes the relay transmit power and the coefficients α_j satisfy the conditions:

$$\sum_{j=1}^{2} \alpha_j = 1, \quad \alpha_1 > \alpha_2$$

leading to

$$|h_{1.R_i D}|^2 < |h_{2.R_i D}|^2 .$$

The signal received by the UE$_j$ users can be expressed as follows:

$$y_j = \left(\rho \widehat{\widetilde{h}}^{(\tau)}_{j.R_i D} + e_{II} \right) \sum_{j=1}^{2} \sqrt{P_r \alpha_j} x_j + n_j \,, \tag{8}$$

where P_r denotes the relay transmit power, n_j is the additive white Gaussian noise (AWGN) $n_j \sim CN\left(0, N_o\right)$.

The received SINRs for x_1 and x_2 at UE$_j$ are defined as:

$$\gamma_1^{R_i D} = \frac{\alpha_1 \gamma_0 \left| \widehat{\widetilde{h}}^{(\tau)}_{1.R_i D} \right|^2}{\alpha_2 \gamma_0 \left| \widehat{\widetilde{h}}^{(\tau)}_{1.R_i D} \right|^2 + \frac{\gamma_0}{\rho_{II}^2} \left(\sigma_{\kappa_{II}}^2 + \sigma_{fd_{II}}^2 \right) + \frac{1}{\rho_{II}^2}}, \tag{9}$$

$$\gamma_{2\to 1}^{R_i D} = \frac{\alpha_1 \gamma_0 \left| \widehat{\widetilde{h}}^{(\tau)}_{2.R_i D} \right|^2}{\alpha_2 \gamma_0 \left| \widehat{\widetilde{h}}^{(\tau)}_{2.R_i D} \right|^2 + \frac{\gamma_0}{\rho_{II}^2} \left(\sigma_{\kappa_{II}}^2 + \sigma_{fd_{II}}^2 \right) + \frac{1}{\rho_{II}^2}}, \tag{10}$$

and

$$\gamma_2^{R_i D} = \frac{\alpha_2 \gamma_0 \left| \widehat{\widetilde{h}}^{(\tau)}_{2.R_i D} \right|^2}{\alpha_1 \gamma_0 \xi \left| \widehat{\widetilde{h}}^{(\tau)}_{2.R_i D} \right|^2 + \frac{\gamma_0}{\rho_{II}^2} \left(\sigma_{\kappa_{II}}^2 + \sigma_{fd_{II}}^2 \right) + \frac{1}{\rho_{II}^2}}, \tag{11}$$

where $\gamma_0 = \frac{P_r}{N_0}$ is the transmit SNR.

3. Performance Analysis

In this section, we derive the OP and throughput expressions of the CNOMA based RS and TAS protocol in the presence of practical impairments, then SIC, CEE, and feedback delay over the Rayleigh fading channel.

3.1. Outage Probability Analysis at Far User

The OP of the CNOMA can be obtained as:

$$P_{e2e.j} = 1 - \left(1 - P_{out.j.I}\right)\left(1 - P_{out.j.II}\right), \tag{12}$$

where $P_{out.j.I}$ and $P_{out.j.II}$ are the OP for the first and second hops, respectively, for each user.

The end-2-end (e2e) OP of UE$_1$ is expressed as follows:

$$P_{e2e.1} = 1 - \left(1 - \Pr\left(\gamma_1^{SR} < \gamma_{th,1}\right)\right)\left(1 - \Pr\left(\gamma_1^{RD} < \gamma_{th,1}\right)\right). \tag{13}$$

In context of best relay selection, the e2e OP for the far user in CNOMA considering both BRS and TAS schemes is expressed as:

$$\begin{aligned} P_{e2e.1}^{BRS} \;=\; & 1 - \prod_{i=1}^{N} \left(1 - \prod_{t=1}^{N_t} \Pr\left(\gamma_1^{SR_i} < \gamma_{th,1}\right) \right) \\ & \times \prod_{i=1}^{N} \left(1 - \prod_{t=1}^{N_t} \Pr\left(\gamma_1^{R_i D} < \gamma_{th,1}\right) \right). \end{aligned} \tag{14}$$

The OP for the first and second hops for UE$_1$ can be calculated as in [31]:

$$\prod_{t=1}^{N_t} \Pr\left(\gamma_1^{SR_i} < \gamma_{th,1}\right) = \prod_{t=1}^{N_t} \left(1 - \exp \frac{\lambda_1^{SR_i}}{\sigma_{1.SR_i}^2} \right), \tag{15}$$

and

$$\prod_{t=1}^{N_t} \Pr\left(\gamma_1^{R_i D} < \gamma_{th,1}\right) = \prod_{t=1}^{N_t} \left(1 - \exp \frac{\lambda_1^{R_i D}}{\sigma_{1.R_i D}^2}\right), \quad (16)$$

where:

$$\lambda_1^{SR_i} = \frac{\frac{\gamma_{th,1}}{\rho_I^2}\left(1+\gamma_0\left(\sigma_{\kappa_I}^2+\sigma_{fd_I}^2\right)\right)}{\gamma_0\left(\alpha_1-\alpha_2\gamma_{th,1}\right)},$$
$$\lambda_1^{R_i D} = \frac{\frac{\gamma_{th,1}}{\rho_I^2}\left(1+\gamma_0\left(\sigma_{\kappa_{II}}^2+\sigma_{fd_{II}}^2\right)\right)}{\gamma_0\left(\alpha_1-\alpha_2\gamma_{th,1}\right)}.$$

Finally, by substituting Eqs. (15) and (16) into (14), the end-to-end OP of the far user can be expressed as:

$$P_{e2e.1}^{BRS} = 1 - \prod_{i=1}^{N}\left(1 - \prod_{t=1}^{N_t}\left(1 - \exp \frac{\lambda_1^{SR_i}}{\sigma_{1.r}^2}\right)\right) \times \prod_{i=1}^{N}\left(1 - \prod_{t=1}^{N_t}\left(1 - \exp \frac{\lambda_1^{R_i D}}{\sigma_1^2}\right)\right). \quad (17)$$

In context of partial relay selection, the e2e OP for the far user in CNOMA incorporating both PRS at first hop and TAS schemes is formulated as:

$$P_{e2e.1}^{PRS} = 1 - \left(1 - \prod_{i=1}^{N}\prod_{t=1}^{N_t} \Pr\left(\gamma_1^{SR_i} < \gamma_{th.1}\right)\right) \times \left(1 - \prod_{t=1}^{N_t} \Pr\left(\gamma_1^{R_s D} < \gamma_{th.1}\right)\right). \quad (18)$$

By substituting $\lambda_1^{SR_i}$ and $\lambda_1^{R_s D}$ into Eq. (18), the end-to-end OP for the far user, considering TAS and PRS, can be expressed as:

$$P_{e2e.1}^{PRS} = 1 - \left(1 - \prod_{i=1}^{N}\prod_{t=1}^{N_t}\left(1 - \exp \frac{\lambda_1^{SR_i}}{\sigma_{1.SR_i}^2}\right)\right) \times \left(1 - \prod_{t=1}^{N_t}\left(1 - \exp \frac{\lambda_1^{R_s D}}{\sigma_{1.R_s D}^2}\right)\right). \quad (19)$$

3.2. Outage Probability Analysis at Near User

We recall that the e2e OP of CNOMA for the near user is:

$$P_{e2e.2} = 1 - \left(1 - \Pr\left(\gamma_2^{SR} < \gamma_{th,2}\right)\right)\left(1 - \Pr\left(\gamma_2^{RD} < \gamma_{th,2}\right)\right). \quad (20)$$

In the best relay selection, the e2e OP for the near user in CNOMA considering both BRS and TAS schemes is expressed as:

$$P_{e2e.2}^{BRS} = \prod_{i=1}^{N}\left(1 - \left(1 - \underbrace{\prod_{t=1}^{N_t} P_{out.2}^{SR_i}}_{term\ I}\right)\left(1 - \underbrace{\prod_{t=1}^{N_t} P_{out.2}^{R_i D}}_{term\ II}\right)\right), \quad (21)$$

In this context, terms I and II denote the OP of the near user utilizing the TAS protocol in the first and second hops, respectively. Therefore, the OP of the term I for UE_2, can be expressed as:

$$\prod_{t=1}^{N_t} P_{out.2}^{SR_i} = \prod_{t=1}^{N_t} P\left(\gamma_{2\to1}^{SR_i} < \gamma_{th.1}\right) + \left[\prod_{t=1}^{N_t} P\left(\gamma_{2\to1}^{SR_i} \geqslant \gamma_{th.1}\right)\prod_{t=1}^{N_t} P\left(\gamma_2^{SR_i} < \gamma_{th.2}\right)\right]. \quad (22)$$

Each probability condition is calculated as:

$$\prod_{t=1}^{N_t} P\left(\gamma_{2\to1}^{SR_i} < \gamma_{th.1}\right) = \prod_{t=1}^{N_t}\left(1 - \exp -\frac{\lambda_2^{SR_i}}{\sigma_{2,SR_i}^2}\right), \quad (23)$$

and

$$\prod_{t=1}^{N_t} P\left(\gamma_2^{SR_i} < \gamma_{th.2}\right) = \prod_{t=1}^{N_t}\left(1 - \exp -\frac{\lambda_3^{SR_i}}{\sigma_{2,SR_i}^2}\right), \quad (24)$$

where:

$$\lambda_2^{SR_i} = \frac{\frac{\gamma_{th_1}}{\rho_I^2}\left(1+\gamma_0\left(\sigma_{\kappa_I}^2+\sigma_{fd_I}^2\right)\right)}{\gamma_0\left(\alpha_1-\alpha_2\gamma_{th_1}\right)},$$
$$\lambda_3^{SR_i} = \frac{\frac{\gamma_{th_2}}{\rho_I^2}\left(1+\gamma_0\left(\sigma_{\kappa_I}^2+\sigma_{fd_I}^2\right)\right)}{\gamma_0\left(\alpha_2-\alpha_1\xi\gamma_{th_2}\right)}.$$

After substituting Eqs. (23) and (24) into (22), the term I can be written as:

$$\prod_{t=1}^{N_t} P_{out.2}^{SR_i} = \prod_{t=1}^{N_t}\left(1 - \exp -\frac{\lambda_2^{SR_i}}{\sigma_{2,SR_i}^2}\right) + \left(1 - \prod_{t=1}^{N_t}\left(1 - \exp -\frac{\lambda_2^{SR_i}}{\sigma_{2,SR_i}^2}\right)\right) \times \prod_{t=1}^{N_t}\left(1 - \exp -\frac{\lambda_3^{SR_i}}{\sigma_{2,SR_i}^2}\right). \quad (25)$$

Similarly to the first hop, the OP of the second hop for UE_2, can be expressed as follows:

$$\prod_{t=1}^{N_t} P_{out.2}^{R_i D} = \prod_{t=1}^{N_t} P\left(\gamma_{2\to1}^{R_i D} < \gamma_{th.1}\right) + \left[\prod_{t=1}^{N_t} P\left(\gamma_{2\to1}^{R_i D} \geqslant \gamma_{th.1}\right)\prod_{t=1}^{N_t} P\left(\gamma_2^{R_i D} < \gamma_{th.2}\right)\right]. \quad (26)$$

The calculation of each probability condition is as follows:

$$\prod_{t=1}^{N_t} P\left(\gamma_{2\to1}^{R_i D} < \gamma_{th.1}\right) = \prod_{t=1}^{N_t}\left(1 - \exp -\frac{\lambda_2^{R_i D}}{\sigma_{2,R_i D}^2}\right), \quad (27)$$

$$\prod_{t=1}^{N_t} P\left(\gamma_2^{R_i D} < \gamma_{th.2}\right) = \prod_{t=1}^{N_t}\left(1 - \exp -\frac{\lambda_3^{R_i D}}{\sigma_{2,R_i D}^2}\right), \quad (28)$$

where:

$$\lambda_2^{R_i D} = \frac{\frac{\gamma_{th_1}}{\rho_{II}^2}\left(1+\gamma_0\left(\sigma_{\kappa_{II}}^2+\sigma_{fd_{II}}^2\right)\right)}{\gamma_0\left(\alpha_1-\alpha_2\gamma_{th_1}\right)},$$
$$\lambda_3^{R_i D} = \frac{\frac{\gamma_{th_2}}{\rho_{II}^2}\left(1+\gamma_0\left(\sigma_{\kappa_{II}}^2+\sigma_{fd_{II}}^2\right)\right)}{\gamma_0\left(\alpha_2-\alpha_1\xi\gamma_{th_2}\right)}.$$

Now, by substituting Eqs. (27) and (28) into (26), the term II can be obtained as:

$$\begin{aligned}\prod_{t=1}^{N_t} P_{out.2}^{R_iD} &= \prod_{t=1}^{N_t}\left(1-\exp-\frac{\lambda_2^{R_iD}}{\sigma^2_{2,R_iD}}\right)\\ &+\left(1-\prod_{t=1}^{N_t}\left(1-\exp-\frac{\lambda_2^{R_iD}}{\sigma^2_{2,R_iD}}\right)\right)\\ &\times\prod_{t=1}^{N_t}\left(1-\exp-\frac{\lambda_3^{R_iD}}{\sigma^2_{2,R_iD}}\right).\end{aligned} \tag{29}$$

Finally, the e2e OP of the UE_2 using TAS and BRS is obtained by substituting Eqs. (25) and (29) into Eq. (21).

In line with the proofs presented previously, for partial relay selection the e2e OP for the near user in CNOMA using both PRS and TAS schemes is obtained as:

$$P_{e2e.2}^{PRS} = 1-\left(1-\prod_{i=1}^{N}\prod_{t=1}^{N_t}P_{out.2}^{SR_i}\right)\left(1-\prod_{t=1}^{N_t}P_{out.2}^{R_sD}\right), \tag{30}$$

where:

$$\begin{aligned}\prod_{t=1}^{N_t} P_{out.2}^{R_sD} &= \prod_{t=1}^{N_t} P\left(\gamma_{2\to1}^{R_sD}<\gamma_{th.1}\right)\\ &+\left[\prod_{t=1}^{N_t} P\left(\gamma_{2\to1}^{R_sD}\geqslant\gamma_{th.1}\right)\prod_{t=1}^{N_t} P\left(\gamma_{2}^{R_sD}<\gamma_{th.2}\right)\right].\end{aligned} \tag{31}$$

Following the same mathematical proofs:

$$\begin{aligned}\prod_{t=1}^{N_t} P_{out.2}^{R_sD} &= \prod_{t=1}^{N_t}\left(1-\exp-\frac{\lambda_2^{R_sD}}{\sigma^2_{2,R_sD}}\right)\\ &+\left(1-\prod_{t=1}^{N_t}\left(1-\exp-\frac{\lambda_2^{R_sD}}{\sigma^2_{2,R_sD}}\right)\right)\\ &\times\prod_{t=1}^{N_t}\left(1-\exp-\frac{\lambda_3^{R_sD}}{\sigma^2_{2,R_sD}}\right).\end{aligned} \tag{32}$$

Finally, the e2e OP of the UE_2 using TAS and PRS is obtained by substituting Eqs. (25) and (32) into Eq. (30).

3.3. Asymptotic Outage Probability

In this subsection, we analyze the performance of asymptotic OP in scenarios marked by high SNR, aiming to gain a more profound understanding of the considered situations. Hence, the asymptotic OP is defined in conditions of high SNR (i.e. as $\gamma_0\to\infty$), employing the McLaurin series expansion [32] $e^{-x}\approx 1-x$.

The asymptotic expression for the OP of far user of UE_1, at high SNR regime is given for BRS and PRS scenarios, respectively, as:

$$\begin{aligned}P_{e2e.1}^{BRS,asy} &\approx 1-\prod_{i=1}^{N}\left(1-\prod_{t=1}^{N_t}\frac{\lambda_1^{SR_i}}{\sigma^2_{1.SR_i}}\right)\\ &\times\prod_{i=1}^{N}\left(1-\prod_{t=1}^{N_t}\frac{\lambda_1^{R_iD}}{\sigma^2_{1.R_iD}}\right)\end{aligned} \tag{33}$$

and

$$\begin{aligned}P_{e2e.1}^{PRS,asy} &\approx 1-\left(1-\prod_{i=1}^{N}\prod_{t=1}^{N_t}\frac{\lambda_1^{SR_i}}{\sigma^2_{1.SR_i}}\right)\\ &\times\left(1-\prod_{t=1}^{N_t}\frac{\lambda_1^{R_sD}}{\sigma^2_{1.R_sD}}\right).\end{aligned} \tag{34}$$

Similarly, the asymptotic expression for the OP of near user of UE_2, at high SNR regime is given for BRS and PRS scenarios, respectively, as follows:

$$\begin{aligned}\prod_{t=1}^{N_t} P_{out.2}^{SR_i,asy} &\approx \prod_{t=1}^{N_t}\frac{\lambda_2^{SR_i}}{\sigma^2_{2,SR_i}}\\ &+\left[\left(1-\prod_{t=1}^{N_t}\frac{\lambda_2^{SR_i}}{\sigma^2_{2,SR_i}}\right)\times\prod_{t=1}^{N_t}\frac{\lambda_3^{SR_i}}{\sigma^2_{2,SR_i}}\right],\end{aligned} \tag{35}$$

$$\begin{aligned}\prod_{t=1}^{N_t} P_{out.2}^{R_iD,asy} &\approx \prod_{t=1}^{N_t}\frac{\lambda_2^{R_iD}}{\sigma^2_{2,R_iD}}\\ &+\left[\left(1-\prod_{t=1}^{N_t}\frac{\lambda_2^{R_iD}}{\sigma^2_{2,R_iD}}\right)\times\prod_{t=1}^{N_t}\frac{\lambda_3^{R_iD}}{\sigma^2_{2,R_iD}}\right],\end{aligned} \tag{36}$$

and

$$\begin{aligned}\prod_{t=1}^{N_t} P_{out.2}^{R_sD,asy} &\approx \prod_{t=1}^{N_t}\frac{\lambda_2^{R_sD}}{\sigma^2_{2,R_sD}}\\ &+\left[\left(1-\prod_{t=1}^{N_t}\frac{\lambda_2^{R_sD}}{\sigma^2_{2,R_sD}}\right)\times\prod_{t=1}^{N_t}\frac{\lambda_3^{R_sD}}{\sigma^2_{2,R_sD}}\right].\end{aligned} \tag{37}$$

3.4. System Throughput Analysis

The system throughput is the sum of the achievable received bit rates at UE_1 and UE_2. As a result, the system throughput can be calculated as:

$$Tp_{sys} = Tp_1+Tp_2 = (1-P_{out.1})\,R_1^*+(1-P_{out.2})\,R_2^*, \tag{38}$$

where R_1^* and R_2^* are the threshold rates of UE_1 and UE_2, respectively.

4. Numerical Results

In this section, we present validation of the analysis for CNOMA scenarios provided in the previous sections.

The practical impairments, SIC, CEE, and feedback delay, are taken into account to evaluate OP and throughput over the Rayleigh fading channels. With power coefficients allocated as $\alpha_1 = 0.8$ and $\alpha_2 = 0.2$, the distance between the BS and relays set to $dsr = 1$ m and distances between the users and relays set to $dr_1 = 2$ m and $dr_2 = 1$ m.

Additionally, we have $\xi = 0.01$, $\sigma_\kappa^2 = 0.01$, and $f_d\tau = 0.02$. In the plots, different lines and markers represent analytical, simulation, and asymptotic curves. The figures demonstrate a close alignment among the analytical, asymptotic, and simulated results, providing strong confirmation of the validity of the performance analysis.

The analytical and simulation results in Figs. 2-5 compare multiple scenarios inside the downlink CNOMA system, examining the OP of UE_1 and UE_2, separately. These scenarios include the use of AS and RS to CNOMA while considering

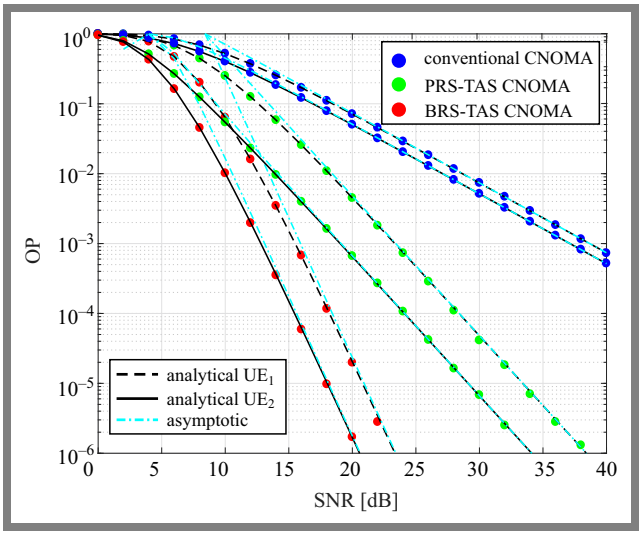

Fig. 2. OP of the downlink CNOMA scenarios under ideal conditions.

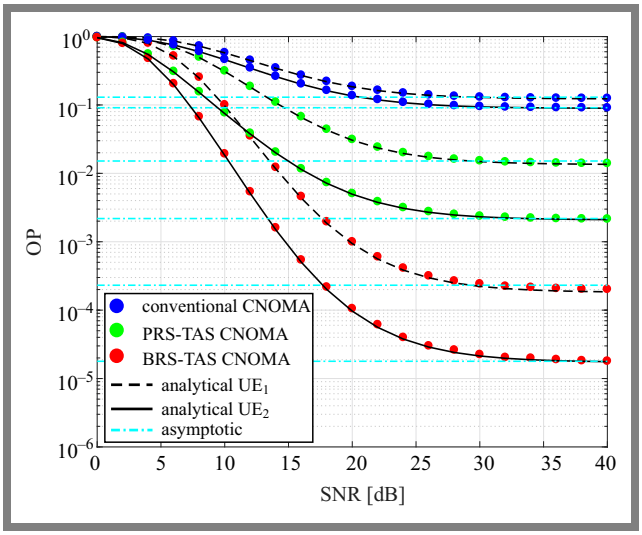

Fig. 3. OP of the downlink CNOMA scenarios under impaired conditions.

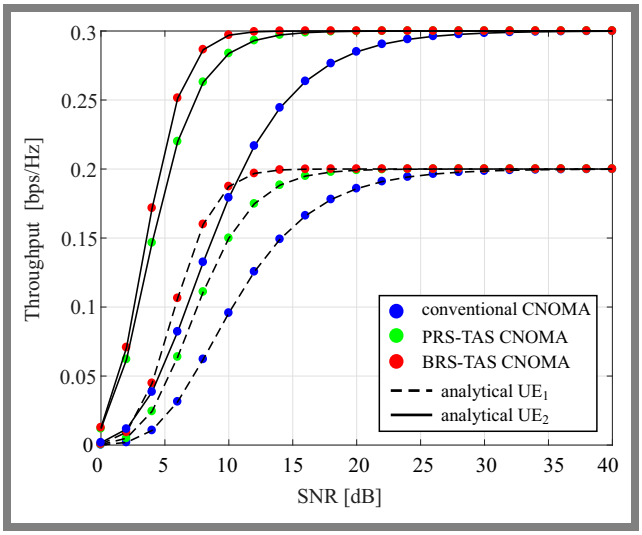

Fig. 4. Throughput of the downlink CNOMA scenarios under ideal conditions.

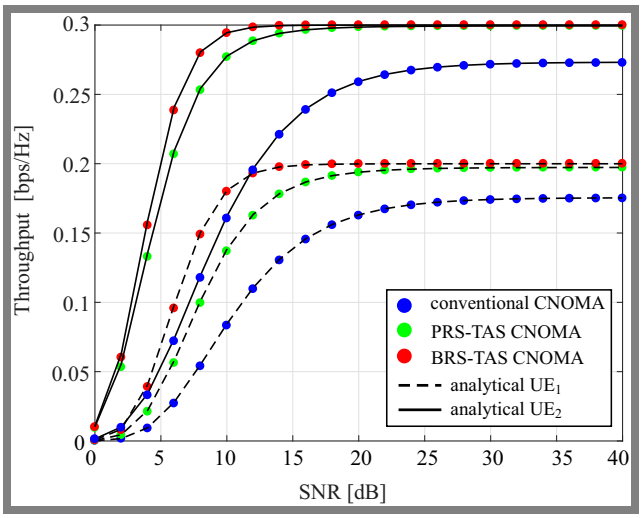

Fig. 5. Throughput of the downlink CNOMA scenarios under impaired conditions.

the presence and absence of certain impairments: $\xi = 0.01$, $\sigma_\kappa^2 = 0.01$, and $f_d\tau = 0.02$.

Figures 2 and 3 depict the OP outcomes at UE_1 and UE_2 for various scenarios, including conventional CNOMA using a single antenna, and one relay as a benchmark, and TAS integration into CNOMA-based PRS and BRS. Through analysis and simulation, it becomes evident that the performance of the CNOMA system gradually improves with the addition of more RS.

Moreover, employing the TAS protocol at both the BS and relays yields better performance than relying only on conventional CNOMA. This underscores the significance of antenna configurations at the BS and relays for enhancing CNOMA system performance.

However, as depicted in Fig. 3, there is a decline in performance attributed to the presence of imperfections in SIC, CEE and feedback delay, leading to an error floor at high SNR.

Also, Figs. 2 and 3 provide insights into the OP of UE_1, and UE_2. Notably, the CNOMA-based BRS-TAS scenario demonstrates superior performance compared to other scenarios. This enhancement is achieved by incorporating TAS at both the BS and relays, confirming the critical role of leveraging multiple antennas for improved users performance.

In addition, the asymptotic results closely align with the analytical findings, validating the accuracy and reliability of our analysis.

In Figs. 4 and 5, we present the throughput performance comparison of the studied scenarios versus SNR, considering the presence and absence of imperfections in SIC, CEE, and feedback delay. As we can see, the PRS-TAS CNOMA outperforms conventional CNOMA. While the BRS-TAS CNOMA has a positive impact compared to counterparts PRS-TAS CNOMA.

The simulation plots are well-matched with the analytical results, validating the accuracy of our analysis.

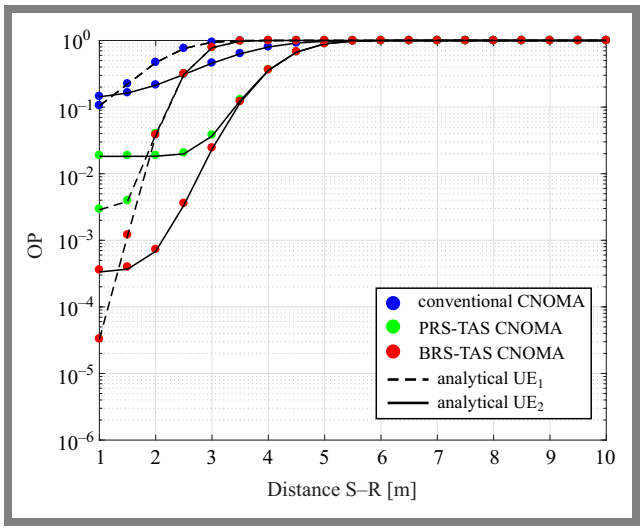

Fig. 6. The impact of distance on the OP of the downlink CNOMA under various impairments.

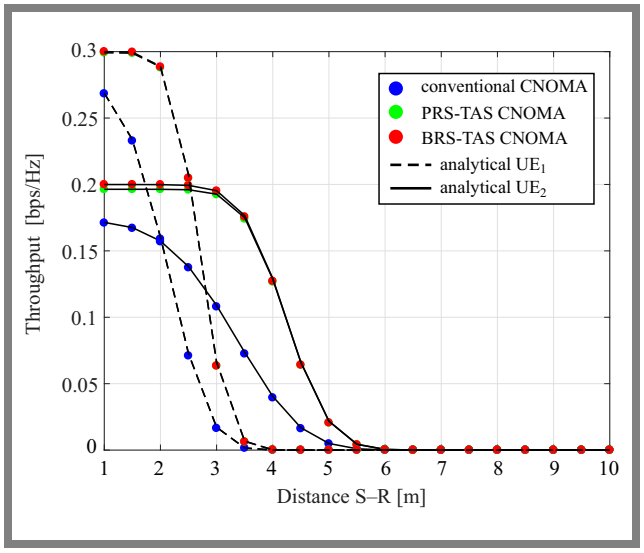

Fig. 7. The impact of distance on the throughput of the downlink CNOMA under various impairments.

Figures 6 and 7, depict the OP and throughput of the CNOMA system relative to the distance dr, assuming an SNR of 25 dB. Specifically, we compare the performance of CNOMA with BRS-TAS against conventional CNOMA.

Noteworthy observations lead to several conclusions. At $dr = 1$ m, UE_2 exhibits superior OP performance compared to the far user UE_1. However, at distances $dr = 2$ m and beyond, the performance of UE_1 surpasses that of UE_2. Furthermore, as the distance increases, UE_2 experiences outage more rapidly than UE_1.

The assessment of the influence of power allocation α_1 on CNOMA is conducted by examining the OP and throughput in Figs. 8 and 9, respectively. With a fixed SNR of 25 dB, it is evident that the performance of UE_1 improves proportionally with the increased power allocated to it.

However, this improvement comes at the expense of deteriorating performance for UE_2.

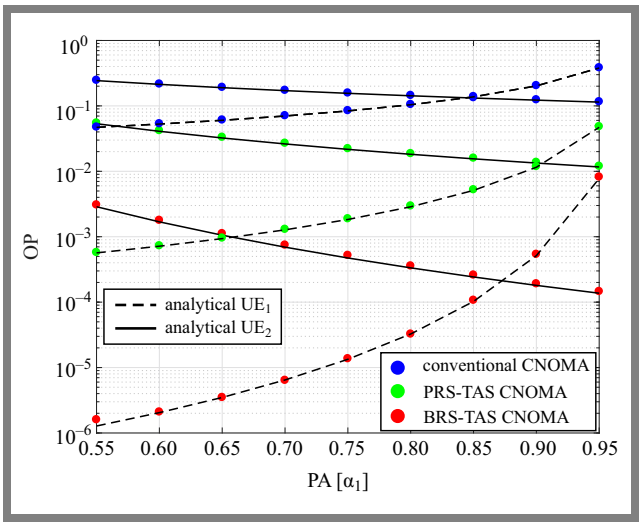

Fig. 8. The impact of PA on the OP of the downlink CNOMA under various impairments.

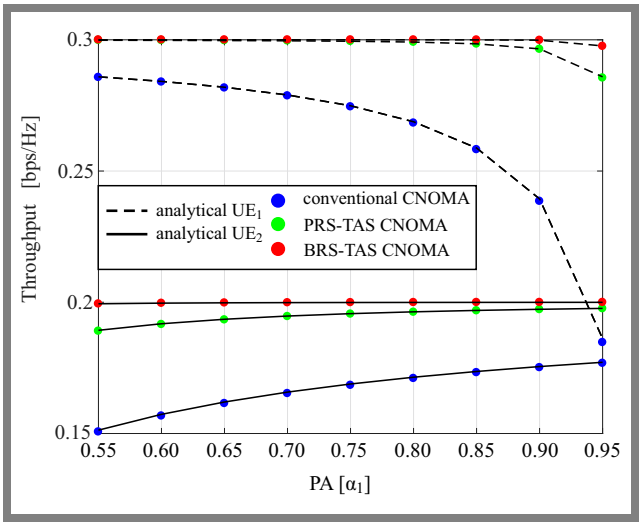

Fig. 9. The impact of PA on the throughput of the downlink CNOMA under various impairments.

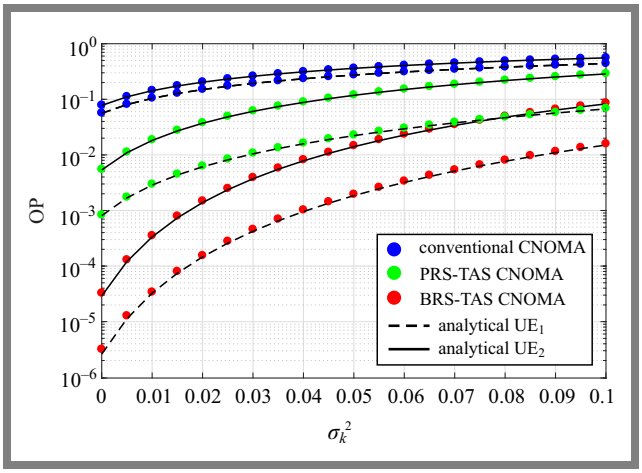

Fig. 10. The impact of CEE on the OP of the downlink CNOMA under various impairments.

Furthermore, it is notable that, across varying values of α_1, the CNOMA-based BRS-TAS consistently ensures superior performance in both OP and throughput.

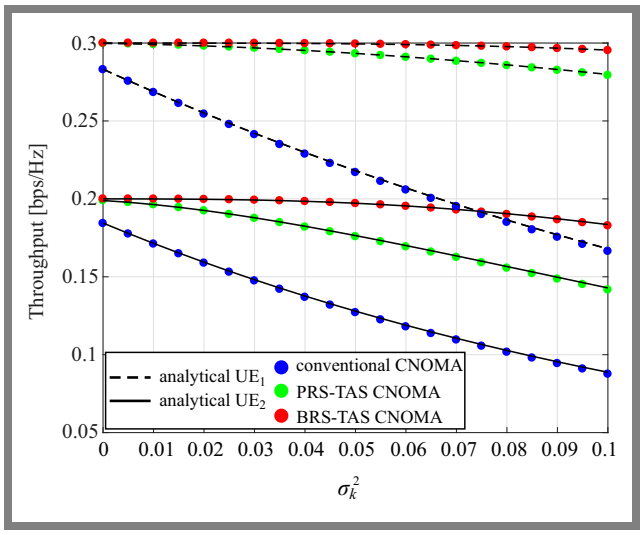

Fig. 11. The impact of CEE on the throughput of the downlink CNOMA under various impairments.

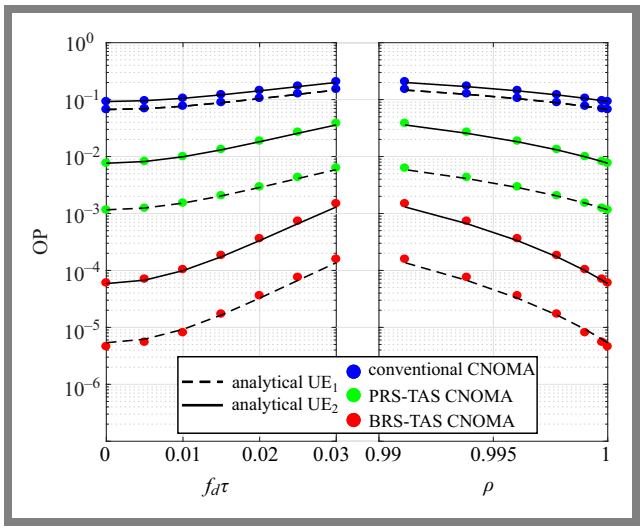

Fig. 12. The impact of ρ and $f_d\tau$ on the OP of the downlink CNOMA under various impairments.

The channel estimation error σ_κ^2 exerts a detrimental impact on the OP and throughput across all CNOMA scenarios. This adverse effect becomes more pronounced with an escalation in the degree of the error, as illustrated in Figs. 10 and 11.

Figures 12 and 13, depict the influence of feedback delay and time correlation coefficient ρ on the OP and throughput of the CNOMA system. Maintaining a constant SNR at 25 dB, it is evident that an increase in feedback delay results in a degradation of the system's performance, both in terms of OP and throughput. Conversely, higher values of ρ contribute to an enhancement in performance.

5. Conclusions

In conclusion, this paper systematically explored and compared CNOMA with TAS against the conventional CNOMA approach. The investigation considered both BRS and PRS paradigm selection among multiple relays, resulting in the

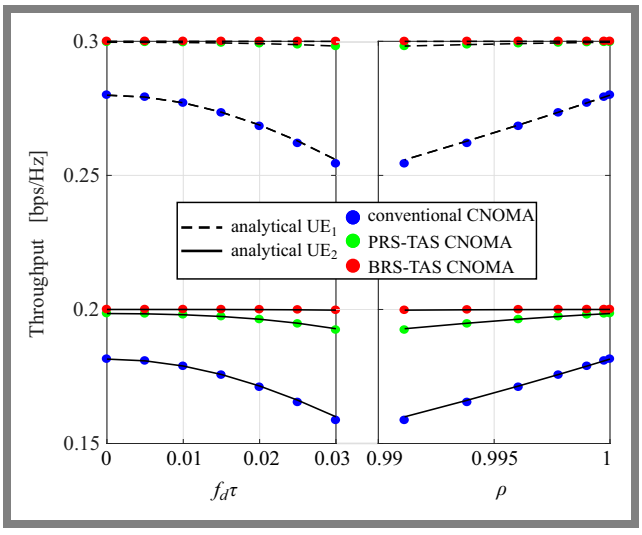

Fig. 13. The impact of ρ and $f_d\tau$ on the throughput of the downlink CNOMA under various impairments.

formulation of BRS-TAS CNOMA and PRS-TAS CNOMA schemes. Practical impairments such as SIC error, CEE, and feedback delay were comprehensively considered in both scenarios. Exact expressions for OP and throughput over Rayleigh fading channels were derived and validated through simulations and asymptotic proofs.

The findings underscored that augmenting the number of antennas at the BS or relays significantly improves the overall performance of CNOMA schemes. Furthermore, the incorporation of a relay selection paradigm yielded additional enhancements in system performance. Importantly, the adverse effects of impairments were alleviated through the strategic application of selection criteria for antennas and/or relays.

In summary, the alignment between analytical, asymptotic, and simulated results establishes the robustness and accuracy of the analytical framework presented in this study. These insights contribute to advancing the understanding of selection strategies in CNOMA systems, with implications for optimizing performance in practical communication scenarios.

References

[1] H. Tullberg *et al.*, "The METIS 5G System Concept: Meeting the 5G Requirements", *IEEE Communications Magazine*, vol. 54, no. 12, pp. 132–139, 2016 (https://doi.org/10.1109/MCOM.2016.1500799CM).

[2] W. Shin *et al.*, "Non-orthogonal Multiple Access in Multi-cell Networks: Theory, Performance, and Practical Challenges", *IEEE Communications Magazine*, vol. 55, no. 10, pp. 176–183, 2017 (https://doi.org/10.1109/MCOM.2017.1601065).

[3] B. Selim *et al.*, "Radio-frequency Front-end Impairments: Performance Degradation in Non-orthogonal Multiple Access Communication Systems", *IEEE Vehicular Technology Magazine*, vol. 14, no. 1, pp. 89–97, 2019 (https://doi.org/10.1109/MVT.2018.2867646).

[4] Z. Yang, Z. Ding, P. Fan, and N. Al-Dhahir, "A General Power Allocation Scheme to Guarantee Quality of Service in Downlink and Uplink NOMA Systems", *IEEE Transactions on Wireless Communications*, vol. 15, no. 11, pp. 7244–7257, 2016 (https://doi.org/10.1109/TWC.2016.2599521).

[5] H. Liu *et al.*, "Decode-and-forward Relaying for Cooperative NOMA Systems with Direct Links", *IEEE Transactions on Wireless Communications*, vol. 17, no. 12, pp. 8077–8093, 2018 (https://doi.org/10.1109/TWC.2018.2873999).

[6] G. Li, D. Mishra, and H. Jiang, "Cooperative NOMA with Incremental Relaying: Performance Analysis and Optimization", *IEEE Transactions on Vehicular Technology*, vol. 67, no. 11, pp. 11291–11295, 2018. (https://doi.org/10.1109/TVT.2018.2869531).

[7] A. Tregancini, *et al.*, "Performance Analysis of Full-duplex Relay-aided NOMA Systems Using Partial Relay Selection", *IEEE Transactions on Vehicular Technology*, vol. 69, no. 1, pp. 622–635, 2019 (https://doi.org/10.1109/TVT.2019.2952526).

[8] L. Zhang *et al.*, "Performance Analysis and Optimization in Downlink NOMA Systems with Cooperative Full-duplex Relaying", *IEEE Journal on Selected Areas in Communications*, vol. 35, no. 10, pp. 2398–2412, 2017 (https://doi.org/10.1109/JSAC.2017.2724678).

[9] X. Liang *et al.*, "Outage Performance for Cooperative NOMA Transmission with an AF Relay", *IEEE Communications Letters*, vol. 21, no. 11, pp. 2428–2431, 2017 (https://doi.org/10.1109/LCOMM.2017.2681661).

[10] A.A. Hamza, I. Dayoub, I. Alouani, and A. Amrouche, "On the Error Rate Performance of Full-duplex Cooperative NOMA in Wireless Networks", *IEEE Transactions on Communications*, vol. 70, no. 3, pp. 1742–1758, 2021 (https://doi.org/10.1109/TCOMM.2021.3138079).

[11] X. Yue *et al.*, "Exploiting Full/half-duplex User Relaying in NOMA Systems", *IEEE Transactions on Communications*, vol. 66, no. 2, pp. 560–575, 2017 (https://doi.org/10.1109/TCOMM.2017.2749400).

[12] N. Guo, J. Ge, Q. Bu, and C. Zhang, "Multi-user Cooperative Non-orthogonal Multiple Access Scheme with Hybrid Full/half-duplex User-assisted Relaying", *IEEE Access*, vol. 7, pp. 39207–39226, 2019 (https://doi.org/10.1109/ACCESS.2019.2906382).

[13] V. Aswathi and A. Babu, "Full/half Duplex Cooperative NOMA under Imperfect Successive Interference Cancellation and Channel State Estimation Errors", *IEEE Access*, vol. 7, pp. 179961–179984, 2019 (https://doi.org/10.1109/ACCESS.2019.2959001).

[14] F. Khennoufa, K. Abdellatif, and F. Kara, "Bit Error Rate and Outage Probability Analysis for Multi-hop Decode-and-forward Relay-aided NOMA with Imperfect SIC and Imperfect CSI", *AEU-International Journal of Electronics and Communications*, vol. 147, art. no. 154124, 2022 (https://doi.org/10.1016/j.aeue.2022.154124).

[15] Y. Li *et al.*, "Performance Analysis of Relay Selection in Cooperative NOMA Networks", *IEEE Communications Letters*, vol. 23, no. 4, pp. 760–763, 2019 (https://doi.org/10.1109/LCOMM.2019.2898409).

[16] S. Lee *et al.*, "Non-orthogonal Multiple Access Schemes with Partial Relay Selection", *IET Communications*, vol. 11, no. 6, pp. 846–854, 2017 (https://doi.org/10.1049/iet-com.2016.0836).

[17] J. Ju *et al.*, "Performance Analysis for Cooperative NOMA with Opportunistic Relay Selection", *IEEE Access*, vol. 7, pp. 131488–131500, 2019 (https://doi.org/10.1109/ACCESS.2019.2940969).

[18] T.-T.T. Nguyen *et al.*, "New Look on Relay Selection Strategies for Full-duplex Multiple-relay NOMA over Nakagami-m Fading Channels", *Wireless Networks*, vol. 27, no. 2, pp. 3827–3843, 2021 (https://doi.org/10.1007/s11276-021-02676-1).

[19] H. Lei *et al.*, "Secrecy Outage Analysis for Cooperative NOMA Systems with Relay Selection Schemes", *IEEE Transactions on Communications*, vol. 67, no. 9, pp. 6282–6298, 2019 (https://doi.org/10.1109/TCOMM.2019.2916070).

[20] I. Umakoglu *et al.*, "BER Performance Comparison of AF and DF Assisted Relay Selection Schemes in Cooperative NOMA Systems", *2021 IEEE International Black Sea Conference on Communications and Networking (BlackSeaCom)*, Bucharest, Romania, 2021 (https://doi.org/10.1109/BlackSeaCom52164.2021.9527771).

[21] K. Sultan, "Best Relay Selection Schemes for NOMA Based Cognitive Relay Networks in Underlay Spectrum Sharing", *IEEE Access*, vol. 8, pp. 190160–190172, 2020 (https://doi.org/10.1109/ACCESS.2020.3031631).

[22] S. Sanayei and A. Nosratinia, "Antenna Selection in MIMO Systems", *IEEE Communications Magazine*, vol. 42, no. 10, pp. 68–73, 2004 (https://doi.org/10.1109/MCOM.2004.1341263).

[23] A.P. Shrestha *et al.*, "Performance of Transmit Antenna Selection in Non-orthogonal Multiple Access for 5G Systems", *Eighth International Conference on Ubiquitous and Future Networks*, Vienna, Austria, 2016 (https://doi.org/10.1109/ICUFN.2016.7536954).

[24] A. Dua, K. Medepalli, and A. J. Paulraj, "Receive Antenna Selection in MIMO Systems Using Convex Optimization", *IEEE Transactions on Wireless Communications*, vol. 5, no. 9, pp. 2353–2357, 2006 (https://doi.org/10.1109/TWC.2006.1687757).

[25] S. Menaa *et al.*, "On the Ergodic Capacity of MIMO-NOMA Systems with JTRAS Protocol under Imperfect SIC and CSI", *International Journal of Electronics*, pp. 1–20, 2023 (https://doi.org/10.1080/00207217.2023.2240077).

[26] T-N. Tran and M. Voznak, "On Secure System Performance over SISO, MISO and MIMO- NOMA Wireless Networks Equipped a Multiple Antenna Based on TAS Protocol", *EURASIP Journal on Wireless Communications and Networking*, vol. 2020, no. 1, pp. 1–22, 2020 (https://doi.org/10.1186/s13638-019-1586-y).

[27] M. Mohammadi, Z. Mobini, H.A. Suraweera, and Z. Ding, "Antenna Selection in Full-duplex Cooperative NOMA Systems", *IEEE International Conference on Communications (ICC)*, Kansas City, USA, 2018 (https://doi.org/10.1109/ICC.2018.8422356).

[28] M. Aldababsa *et al.*, "Unified Performance Analysis of Antenna Selection Schemes for Cooperative MIMO-NOMA with Practical Impairments", *IEEE Transactions on Wireless Communications*, vol. 21, no. 6, pp. 4364–4378, 2021 (https://doi.org/10.1109/TWC.2021.3129307).

[29] Y. Yu *et al.*, "Antenna Selection for MIMO Nonorthogonal Multiple Access Systems", *IEEE Transactions on Vehicular Technology*, vol. 67, no. 4, pp. 3158–3171, 2017 (https://doi.org/10.1109/TVT.2017.2777540).

[30] S. Beddiaf *et al.*, "Impact of Hardware Impairment on the Uplink SIMO Cooperative NOMA with Selection Relay under Imperfect CSI", *IEEE Access*, vol. 11, pp. 106706–106721, 2023 (https://doi.org/10.1109/ACCESS.2023.3318932).

[31] S. Singh and M. Bansal, "Outage Analysis of NOMA-based Cooperative Relay Systems with Imperfect SIC", *Physical Communication*, vol. 43, art. no. 101219, 2020 (https://doi.org/10.1016/j.phycom.2020.101219).

[32] S. Lee *et al.*, "Non-orthogonal Multiple Access Schemes with Partial Relay Selection", *IET Communications*, vol. 11, no. 6, pp. 846–854, 2017 (https://doi.org/10.1049/iet-com.2016.0836).

Menaa Saber, Ph.D. student
Department of Electrical Engineering
https://orcid.org/0000-0001-7363-7131
E-mail: menaa-saber@univ-eloued.dz
Echahid Hamma Lakhdar University, El-Oued, Algeria
https://lang.univ-eloued.dz/en/

Khelil Abdellatif, Professor
Department of Electrical Engineering
https://orcid.org/0000-0001-5545-1851
E-mail: abdellatif-khelil@univ-eloued.dz
Echahid Hamma Lakhdar University, El-Oued, Algeria
https://lang.univ-eloued.dz/en/